## A 36×40 Wireless Fluorescence Image Sensor for Real-Time Microscopy in Cancer Therapy

Rozhan Rabbani[1], Hossein Najafiaghdam[1], Biqi Zhao[1], Megan Zeng[1], Vladimir Stojanovic[1], Rikky Muller[1], and Mekhail Anwar[2]

University of California, Berkeley

University of California, San Francisco

Real-time in vivo imaging provides detailed cellular information from targets inside the body. In cancer immunotherapy, for instance, this information can be utilized for early assessments of the treatment, where effective activation of the immune system leads to durable responses against cancer. While only 30% of the patients respond to the treatment, detailed multicellular-level information can help rapidly alter the therapy based on the individual's response. However, this is not possible with current modalities such as CT or MRI that image purely anatomic changes taking months to manifest, by the end of which the window of cure is lost. Moreover, continuous monitoring of the tumor via frequent biopsies is impractical due to the invasiveness of the procedure. To overcome these limitations, fluorescence microscopy can be used to identify multiple cell types within tissue during ongoing therapy.

To implement noninvasive chip-scale fluorescence microscopy, a mm-scale wireless implantable imaging system consisting of an illumination source and an image sensor is required. While state-of-the-art image sensors provide high resolution microscopy, they lack wireless interfaces and require external circuitry making them impractical for chronic real-time *in vivo* monitoring [1,2]. Recent implantable systems have shown power transfer and data communication for low power sensors using ultrasound (US), but they haven't demonstrated wireless power transfer for high-power operations of the SoC such as optical excitation. Here, we present a 36×40 pixel implantable imaging system fabricated in 0.18µm CMOS process for wireless fluorescence microscopy at a depth of 2cm.

Fig. 1 shows the conceptual diagram of the implant consisting of 1) a 1.5×1.5×1.5mm$^3$ piezoceramic (Lead Zirconate Titanate, PZT) 2) an imager ASIC with the pixel array covered by an optical wavelength filter (ET FITC-Cy5, Chroma) 3) a laser diode (CHIP-635-P5, Roithner LaserTechnik) for narrowband excitation of fluorescently-labeled targets and 4) a 1.4mF capacitor to store charge which can be decreased in size by using more efficient optical sources. Previously labeled with injected fluorophore-antibody compounds, the cells excited with the laser diode at 635nm emit light at a wavelength differing by 30nm (Stokes shift). A high-Q bandpass optical filter with a 60dB rejection at the excitation band eliminates bleed-through from the higher intensity (×10$^5$) illumination and background to the emission band. The fluorescence signal intensity is given by $F = \sigma Q P_{in} N$ where $\sigma$, $Q$ and $N$ refer to the absorption cross-section, quantum yield, and the number of fluorophores attached to the target and $P_{in}$ is the incident optical intensity. A 1pW fluorescence signal detectable by the imager in [3], with an average binding of 10$^6$ fluorophores of typical dyes (i.e. Cyanine5.5-NHS), a quantum yield of 20% and an absorption cross-section of $10^{-16}$cm$^2$ requires a high 50 mW/cm$^2$ optical excitation intensity at the absorption peak of the fluorophore with minimum intensity for out of band light. Therefore, a laser diode is chosen to meet both requirements.

The detailed block diagram and timing of the system is shown in Fig. 2. The mote piezo receives the US pulses from an external transducer. An active rectifier converts the US signal to a DC voltage ($V_{RECT}$) and charges the storage capacitor ($C_{store}$) up to 5V. Once $V_{RECT}$ reaches 4.2V, a power on reset (POR) signal is triggered and the finite state machine (FSM) resets to the Charging state. A watchdog signal tracks ultrasound free intervals to navigate state transitions of the FSM run by extracted clock from the US waveform. Upon arrival of the first rising edge of the watchdog, the chip moves to the Imaging state when the laser driver turns on and the pixel array captures the image. Both the laser and the pixel array are switched off after completion of the integration time. 8 integration times from 16-128ms can be hard-coded into the implant. Once the image is captured as described in [3], the pixels are sampled sequentially with a $\Phi_{SEL} = 5\mu s$ control pulse by a differential 8-bit SAR ADC. Multiple LDOs (1V, 1.8V, 2.1V, 2.5V, 3.3V) supply the analog front end, the ADC, the FSM, and the laser driver. For a depth of 2cm, each set of 2 bits is fit inside an interval equal to 2ToF (ToF=14µs, time-of-flight) and is transmitted through On-Off keying (OOK) modulation via US backscattering. A programmable switch with 4 impedance values (1,2,4,8KΩ) sets the modulation depth based on the equivalent impedance of the piezoceramic at the operating frequency.

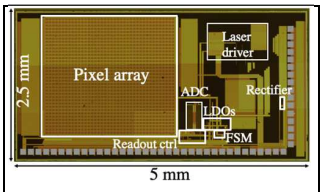

Die micrograph.

Fig. 3a shows state transitions and the 1V droop on $V_{RECT}$ during a 64ms illumination. After illumination, $V_{RECT}$ maintains a voltage higher than 3.5V for ADC and US Backscattering (Fig. 3b). The electro-optical characterization of the laser diode with a power meter (PM100D, Thorlabs) shows an optical power of 3.4mW for a 37mA current and 2.1V forward voltage resulting in an electrical to optical efficiency of 4.4% (Fig. 3c). To avoid overheating the diode, a PWM controller divides the main clock to generate a 50kHz pulse with a 50% duty cycle within the integration time shown in previous work [4]. The distribution of the average optical output power for 20 measurements in Fig. 3d shows an average optical power of 3.5mW (average current of 37.07mA) and an average electrical efficiency of 66% for the laser driver as $V_{RECT}$ is required to be maintained above 3.5V for the operation of the IC after illumination.

The impedance and open circuit voltage of the piezoceramic are characterized inside canola oil as shown in Fig. 4. To achieve maximum harvested voltage, the piezoceramic is operated off-resonance at 960kHz. The spectrum of the harvested voltage is shown for the piezoceramic both off-load and loaded with the equivalent of the IC's input impedance (Fig. 4c). BER for a measurement performed at 2cm of depth inside canola oil with a modulation depth of 16% is $8.7\times10^{-5}$ for 11.52kbits (Fig. 4d).

The measurement setup in Fig.5 consists of the piezoceramic inside a tank of canola oil (0.25 dB/cm/MHz attenuation) connected to the imager. The optical filter is epoxied on the chip and is covered by black epoxy to eliminate any bleed-through from the edges. The on-chip laser driver is connected to the laser diode which illuminates the target from the top. The backscattered images from a Cyanine5.5-NHS fluorophore underneath a USAF resolution target with highlighted corresponding regions are shown in Fig. 5. The images are taken after a 40% duty-cycled 150s Charging state to ensure safe operation of the US transducer. A 64ms illumination with a total readout time of 389ms via US backscatter capture metallic patterns with a single pixel resolution (~55 µm). The frame time is sufficient to capture relatively slow movements of cells inside the body.

This this work is compared against recently published implantable imagers shown in the table in Fig. 6 [1,2,5]. To the best of our knowledge, this is the first wireless implantable fluorescence image sensor that transmits 11.52 kbits of data in a single measurement cycle by supplying the 0.26mW pixel array and the high 78mW power of the laser diode for a 64ms illumination interval. The imaging operation is duty-cycled by 0.04% within a 150.5s frame time resulting in a system overall average power of 55µW per frame.

**Acknowledgement:**

The authors would like to thank National Institute of Health, BSAC, TSMC and Efthymios P Papageorgiou, Mohammad Meraj Ghanbari and Micah Roschelle for support and technical discussions.

**References:**

[1] T. Kobayashi *et al*., "Optical communication with brain cells by means of an implanted duplex micro-device with optogenetics and Ca2+ fluoroimaging". Sci Rep 6, (2016).

[2] J. Choi *et al*., "Fully Integrated Time-Gated 3D Fluorescence Imager for Deep Neural Imaging," in IEEE Transactions on Biomedical Circuits and Systems, Aug. 2020.

[3] E. P. Papageorgiou *et al*., "Chip-Scale Angle-Selective Imager for In Vivo Microscopic Cancer Detection," TBioCAS, 2020.

[4] R. Rabbani *et al*., "Towards an Implantable Fluorescence Image Sensor for Real-Time Monitoring of Immune Response in Cancer Therapy", EMBC, 2021.

[5] A. Sawaby *et al*., "A Wireless Implantable Ultrasound Array Receiver for Thermoacoustic Imaging," VLSI, 2018.

2022 IEEE Custom Integrated Circuits Conference (CICC) | 978-1-6654-0756-4/22/$31.00 ©2022 IEEE | DOI: 10.1109/CICC53496.2022.9772779

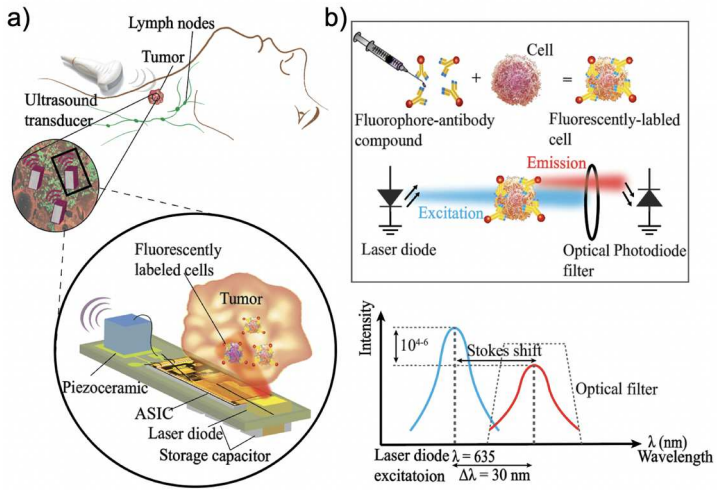


Fig. 1. (a) Conceptual system diagram of the implant (b) fluorescence microscopy for fluorescently-labeled cells

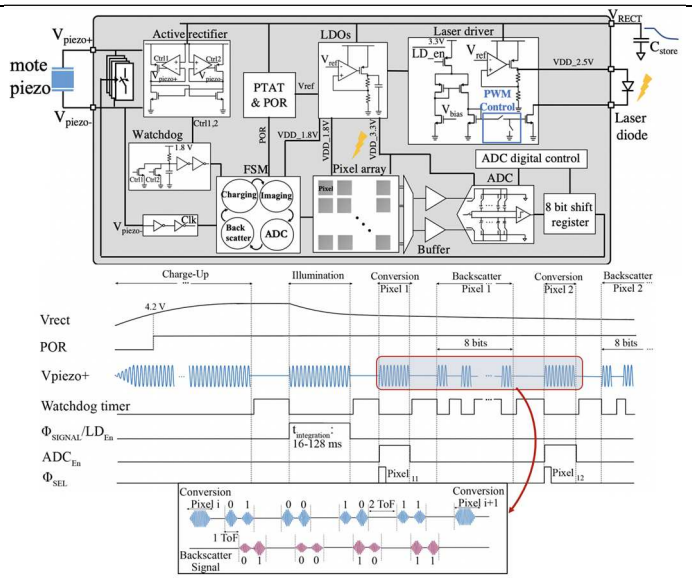


Fig. 2. Schematic and timing diagram of the ASIC

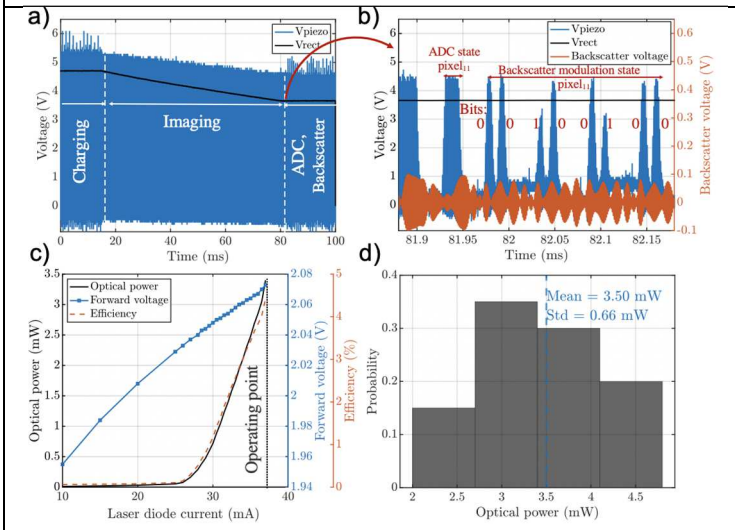


Fig. 3. (a) State transition diagram (b) Detailed ADC and Backscatter state transition per pixel (c) P-I-V characterization of the laser diode (d) Optical power variation for repeated measurements.

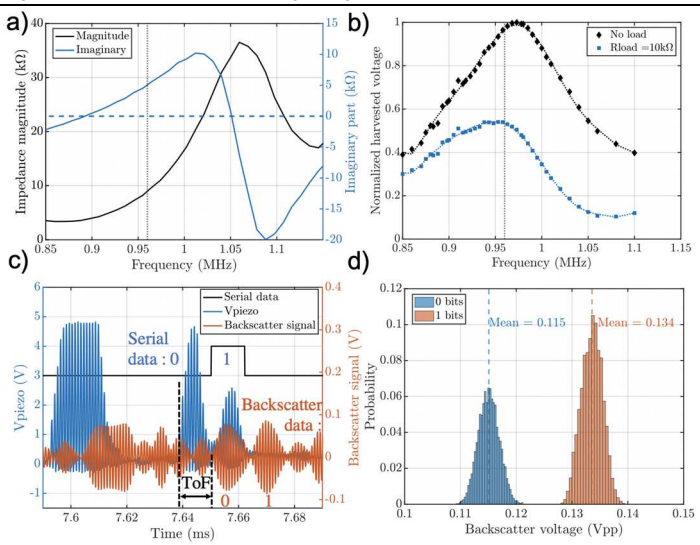


Fig. 4. Frequency spectrum of (a) impedance and (b) harvested voltage of the piezoceramic (c) serial data and backscatter signal with (d) modulation depth of 16% and BER of $8.7\times10^{-5}$

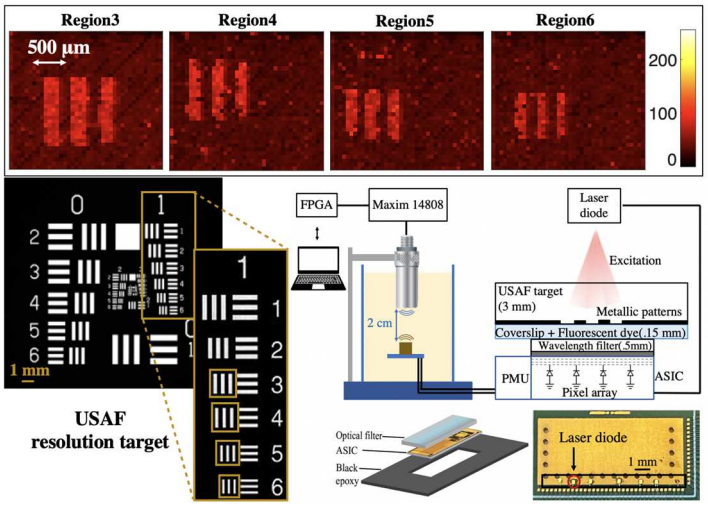


Fig. 5. Backscattered images shown in 8-bit ADC codes and *in vitro* fluorescence microscopy

| | [1] | [2] | [5] | **This work** |
|---|---|---|---|---|
| **Imaging method** | Fluorescence | Fluorescence | Thermoacoustic | **Fluorescence** |
| **Multi-cellular resolution** | Yes | Yes | No | **Yes** |
| **Technology** | 0.35 µm CMOS | 0.13 µm CMOS | 65 nm CMOS | **0.18 µm CMOS** |
| **Wireless** | No | No | Yes | **Yes** |
| **Power source** | Power supply | Power supply | Ultrasound | **Ultrasound** |
| **Array size** | 120 x 268 | 8 x 64 | 1 x 16[a] | **36 x 40** |
| **Pixel size** | 7.5 x 7.5 µm$^2$ | 25.3 x 51.2 µm$^2$ | -- | **55 x 55 µm$^2$** |
| **Excitation time** | -- | 2 ns | 5 µs | **16-128 ms** |
| **Excitation source** | µLED | Laser diode | RF | **Laser diode** |
| **Excitation power** | -- | -- | -- | **3.4 mW** |
| **Implant depth** | -- | -- | 6 cm | **2 cm** |
| **Data transmitted per frame** | Analog | Digital/ 3 kbits | Digital/ 72 [b] kbits | **Digital/ 11.5 kbits** |
| **Imager power** | -- | 14.1 mW | 1.5 mW | **0.26 mW** |
| **System average power per frame (including excitation)** | -- | -- | -- | **0.055 mW** |

[a] Number of CMUT channels [b] Estimated 144 bits based on 9-bit ADC and 16 channels, 72 kbit based on memory size

Fig. 6. Comparison table